Lipid domain separation, bilayer thickening and pearling induced by the cell penetrating peptide penetratin

Antonin Lamazière, Ofelia Maniti, Claude Wolf, Olivier Lambert, Gerard Chassaing, Germain Trugnan, Jesus Ayala-Sanmartin

Lipid domain separation, bilayer thickening and pearling induced by the cell penetrating peptide penetratin

Antonin Lamazière[1,2,3], Ofelia Maniti [1,2,3], Claude Wolf [2], Olivier Lambert [4], Gérard Chassaing [1,2,3], Germain Trugnan [2], and Jesus Ayala-Sanmartin [1,2,3,*]

[1]CNRS, UMR 7203, Laboratoire des BioMolécules, Groupe N. J. Conté, Paris, France.
[2]Université Pierre et Marie Curie, CHU Saint Antoine, Paris, France.
[3]Ecole Normale Supérieure, Département de Chimie, Paris, France
[4]CNRS, UMR 5248, CBMN, Université Bordeaux 1, ENITAB, IECB, Pessac, France.

*Contact. J. Ayala-Sanmartin, Groupe N. J. Conté, CNRS, UMR 7203, 27 rue Chaligny, 75012 Paris, France. e-mail: jesus.ayala-sanmartin@upmc.fr. Tel: 33+1 40 01 13 24. Fax: 33+1 40 01 13 90

Running title: Lipid separation and pearling by penetratin

Abstract

Protein membrane transduction domains are able to translocate through cell membranes. This capacity resulted in new concepts on cell communication and in the design of vectors for internalization of active molecules into cells. Penetratin crosses the plasma membrane by a receptor and metabolic energy-independent mechanism which is at present unknown. A better knowledge of its interaction with phospholipids will help to understand the molecular mechanisms of cell penetration. Here, we investigated the role of lipid composition on penetratin induced membrane perturbations by X-ray diffraction, microscopy and ^{31}P-NMR. Penetratin showed the ability to induce phospholipid domain separation, membrane bilayer thickening, formation of vesicles, membrane undulations and tubular pearling. These data demonstrate its capacity to increase membrane curvature and suggest that dynamic phospholipid-penetratin complexes can be organized in different structural arrangements. These properties and their implications in peptide membrane translocation capacity are discussed.

Keywords: Lipid phase separation; Membrane curvature; Membrane pearling; Membrane thickening; Penetratin; Physical endocytosis.

Abbreviations
Chol, cholesterol; CPP, cell penetrating peptide; GUV, giant unilamellar vesicle; LUV, Large unilamellar vesicle; MLV, multilamellar vesicle; PC, L-α-Phosphatidylcholine; PE, L-α-Phosphatidyl-ethanolamine; PG, L-α-Phosphatidyl-DL-glycerol; R9, nona-arginine peptide; SAXS, small angle X-ray scattering; SM, Sphingomyeline.

1. INTRODUCTION

Cell penetrating peptides (CPP) are potential therapeutic vectors for the delivery of hydrophilic molecules inside eukaryotic cells (for review see [1-3]). These peptides were developed as an alternative approach to other "aggressive" methods to introduce molecules into cells such as trituration [4]. Such peptides (i.e. Tat, penetratin, polyarginine) are usually rich in basic amino acid residues, and some of them are derived from proteins suggesting that they play a role in messenger protein transduction [5]. Penetratin, the transduction domain derived from the homeodomain transcription factor antennapaedia was described as one of the first peptides to successfully carry active molecules inside cells without affecting cell viability and is one of the most studied CPP [6-8].

Different physicochemical parameters are involved in membrane binding and penetration of CPP [9]. In some cases, cell penetration of peptides has been proposed to be independent from receptors and metabolic energy. Direct interaction with membrane lipids seems to be involved in their cellular uptake. Several studies have demonstrated that endocytosis is also involved in the internalization of basic peptides [10]. Recently, Duchardt and collaborators showed that non endocytic and different endocytic mechanisms are involved in the cell penetration of Tat, penetratin and oligoarginine [11]. However, to reach the cytosol and the nucleus, the peptides must escape from the endosome through the endosomal membrane barrier.

The molecular mechanisms of membrane translocation are still debated. Several mechanisms for CPP membrane translocation (plasma membrane or endosomes) have been proposed. These include an “electroporation-like” mechanism [12], neutralization of arginine residues by guanidinium-phosphate complex formation [13, 14], and inverse micelles formation [15] (for reviews see [1, 2, 16]). A recent study has contested the electroporation-like mechanism and has suggested a direct translocation through the bilayer [17]. The formation of pores, a candidate mechanism for internalization of antimicrobial and model amphipathic peptides was excluded for penetratin and highly basic non amphipathic peptides.

Experiments with model membranes have established that peptide translocation in large unilamellar vesicles (LUV) is less efficient than in giant unilamellar vesicles (GUV), [18, 19]. This difference may be related to membrane curvature and/or membrane tension that are higher in LUV than in GUV.

Using membrane models, we have previously shown that penetratin and different basic peptides induce membrane invagination which results in the formation of tubular structures [20]. These invaginations were observed in membranes in the fluid liquid disordered phase [21, 22]. We suggested that membrane curvature induced by basic peptides could be crucial to their mechanisms of internalization. Positive curvature would be necessary to the mechanism of pore formation of amphipathic peptides and negative curvature would be related to the formation of tubes ("physical endocytosis") [20] and inverse micelles. With regards to the protein transduction domains present in several transcription factors (i.e. penetratin), it should be considered their interaction with different phospholipid species. To be internilazed, the basic domain has to be able to interact with the external leaflet of the plasma membrane rich in phosphatidylcholine (PC) and sphingomyeline (SM), and to be secreted with the internal leaflet rich in phosphatidylethanolamine (PE) and negatively charged phospholipids such as phosphatidylserine. Moreover, antimicrobial activity against gram positive and gram negative bacteria suggested the possible interaction of penetratin with PE and phosphatidylglycerol (PG) rich membranes [23].

Herein, to elucidate the mechanism of penetratin actions on phospholipids during intracellular uptake, extracellular export and antimicrobial capacity, the properties of penetratin-phospholipid complexes were studied with phospholipids present in different cellular membranes. We analyzed the penetratin capacity to modify the membrane lipid organization by microscopy, ^{31}P-NMR, X-ray diffraction and cryo-electron microscopy. The results indicate that penetratin is able to induce dynamical phase separation of phospholipid bilayers and membrane thickening as well as an increase in membrane negative curvature resulting in undulations, pearling and vesiculation. The implications of the presented data in penetratin membrane translocation are discussed.

2. MATERIAL AND METHODS

2.1.Materials

Egg L-α-Phosphatidylcholine (PC), egg L-α-Phosphatidyl-DL-glycerol (PG), egg Sphingomyeline (SM), Cholesterol (Chol) and egg L-α-Phosphatidyl-ethanolamine (PE)

were purchased from Sigma. Penetratin (RQIKIWFQNRRMKWKK) and nona-arginine (R9) were synthesized and purified as previously described [20]. The synthesis of 5(6)-Carboxyfluoresceinated penetratin (CF-penetratin) was performed as previously described [21].

2.2. Model membranes

Large unilamellar vesicles (LUV), were prepared with an extrusion device (Avestin) as previously described [24].

Multilamellar vesicles (MLV) for electron microscopy were prepared as follows. 230 µg of a PC solution were dried under a stream of nitrogen and the residual solvent was evaporated under vacuum for an hour. Then 20 µl of buffer A (5 mM HEPES pH 7.4) with or without penetratin (23 µg) were added and gently mixed.

Giant unilamellar vesicles (GUV) were obtained by electroformation as previously described [20]. Briefly, 1.5 µl of lipids solution was spread on platinum electrodes. The lipid films were dried under a gentle stream of nitrogen. The electrodes and the chamber are set on an inverted microscope with a thermocouple monitoring the temperature (25°C). The chamber was filled with 2 ml of buffer A (conductivity 20 µS/cm). Immediately after, a low frequency alternating field (5 Hz and 1 V) was applied on the electrodes for 2 hours. Unless specified in the text, the lipid compositions (by weight) used in this study were, for external leaflet mimicking zwiterionic membranes: PC (pure), PC/chol (4/1), PC/SM/chol (1/1/1). For prokaryotic and internal leaflet negatively charged phospholipids: PC/PG (9/1), PC/PE (2/8), PE (pure).

2.3 Video microscopy

GUV with diameter between 10 to 100 µm were observed by phase contrast microscopy and for CF-penetratin by fluorescence microscopy under exciting illumination (fluo arc N HBO 103, Zeiss) with Zeiss filters (Ex/Em, 546/590+) as previously described [21]. GUVs of diameter between 10 to 100 µm were observed. 2.5 µl of 50 µM peptides solution were added close to the electrodes (2 ml of buffer) and images were captured with a CCD camera (Cool SNAP HQ) controlled with Metamorph software (Roper Scientific).

2.4. ^{31}P-NMR spectroscopy

NMR experiments were recorded on a Bruker DMX 500 spectrometer and processed with the UXNMR software. Measurements were performed at 202.5 MHz, using a single 12.0

μs pulse, followed by 1.2 s relaxation delay time and broadband proton decoupling. Typically, 24 000 scans were accumulated. An exponential multiplication, corresponding to a line broadening of 30 Hz, was applied to FID prior to Fourier transformation. Samples were prepared by dissolving lipids (20 mg) in chloroform/methanol (2/1, vol/vol). The solvent was evaporated under a stream of nitrogen and residual solvent removed under high vacuum for 1 day. In order to obtain the MLV, the dry lipids were hydrated in 1 ml $H_2O/^2H_2O$ (9/1 by vol.) containing 2 mg of penetratin. The experiments were performed at 40°C.

2.5. X ray diffraction

Small angle X-ray scattering (SAXS) measurements were performed at the Synchrotron Radiation Source of Spring8 (Japan) following a protocol adapted from Tessier et al. [25] and described in [21]. Samples were prepared by dissolving dry lipids (20 mg) in chloroform/methanol (2/1, vol/vol) in the indicated proportions. The solvent was subsequently evaporated under a stream of nitrogen at 45°C and residual solvent under high vacuum for 1 day. In order to obtain the fully hydrated (50 wt % water) MLV, the dry lipids were hydrated with 25 μl of buffer A containing 2 mg of penetratin. The lipid dispersion was thoroughly stirred, sealed under argon and kept until examination at 4°C. For X-ray measurements, samples (~20 μl) were deposited between two thin mica windows and mounted on a programmable temperature stage. The sample to detector (Rigaku Image Plate) distance was set to 1 m. Samples were exposed for 30 seconds recording. Spacings were determined from circular integration of 2-D images using FIT2D program (Andy Hammersley) and silver behenate was used as the x axis calibration standard. Peak analysis was performed with Origin and Peakfit 4 programs. The electron density profiles of lipid bilayers were obtained by Fourier synthesis of x-ray diffraction pattern [26]. Integrated densities were derived from three or four diffraction orders by measuring the area under each diffraction peak separated and integrated using the software Peakfit (Seasolve).

2.6. Cryo-Electron microscopy

Penetratin induced membrane perturbations were observed by cryo-electron microscopy of LUV as described in [27] and in PC-MLV. LUV (15 μg) were mixed with 3 μg of penetratin in buffer A and incubated for 15 minutes. LUV incubated with penetratin or MLV prepared as indicated in the 'model membranes' section were vitrified by plunging the

sample into liquid ethane, following a standard fast freeze procedure [28]. Observations were performed with a Tecnai F20 FEI transmission electron microscope, operating at 200 kV. Low-dose images were recorded at a nominal magnification of 50 000 with a USC1000 slow-scan CCD camera (Gatan, CA, USA).

3. RESULTS

3.1. Lamellar phase separation of membrane lipids induced by penetratin

Penetratin and other basic peptides were shown to induce membrane tubulation in giant unilamellar vesicles (GUV) [20, 29, 30]. For penetratin, this effect was dependent on the physical state of the bilayer. The tubulation was inhibited in pure liquid ordered (Lo) state and favored in the liquid disordered (Ld) membranes [21, 22]. Herein, in order to get more insight on the role of the lipid arrangements induced by penetratin, membrane bilayers of different composition were investigated.

The effect of penetratin in PC/SM/Chol (1/1/1) multilamellar vesicles (MLV) at temperatures from 5 to 45°C was studied by small angle X-ray scattering (SAXS). In the absence of peptide at 5°C, a single lamellar phase was assessed by five equally spaced Bragg's peaks (Fig. 1a). The thickness of the bilayer (4.80 nm) and the hydration layer (2.14 nm) were measured by calculating the transversal electron density profile. At 45°C another lamellar phase with a reduced thickness (4.14 nm) was clearly separated (Fig. 1a inset). The increase in temperature resulted in a moderate reduction of the membrane thickness of the first structure (from 4.80 nm at 5°C to 4.51 nm at 45°C, Fig 1b). Cholesterol (Chol) was already described to reduce the decrease in thickness of the bilayer by enhancing the molecular ordering of acyl chains at high temperatures. However the observation above 45°C of the equimolar ternary mixture is consistent with the separation of the liquid ordered and liquid disordered lamellar components. These data is in agreement with previous studies [31] showing at 20°C one lamellar phase with a bilayer thickness of 4.30 nm in dioleoyl-PC/SM/Chol (1/1/1) MLVs, and a separation of two lamellar phases at 37°C (lo of 4.89 nm and ld of 4.52 nm) for PC/brain SM/ Chol [32]. The small differences in these studies are due to the difference in the phospholipid species used. In the first case the authors used the unsaturated dioleoyl-PC and a SM rich in palmitoyl species (C16:0) and in the second case they used brain SM with longer saturated chains (C18:0 and C24:0). In the presence of penetratin, the separation of two lamellar phases with distinct d-spacing was observed from 5°C and remained separated by heating to 45°C. The thicker phase (L1)

behaves similarly with the phase previously observed in the whole temperature range in the absence of penetratin. Characteristically it showed a moderate reduction of thickness with temperature (4.81 nm at 5°C and 4.50 nm at 45°C). The peptide also induced the separation of a second lamellar component (L2) with a strongly temperature-dependent bilayer thickness varying from 4.40 nm at 5°C to 3.75 nm at 45°C (Fig 1b). This component is consistent with a liquid disordered phase in the whole temperature range investigated (Fig. 1b). The peptide seemed to induce vesiculation of membranes as it is suggested by the distorted baseline of the diffractogram which is superimposed between the Bragg's peaks. Phase separation brought about by penetratin was also suggested by other approaches. First, the heterogeneous distribution of fluorescent peptide on PC/PG GUV surface. This transient domains separation was highly dynamic and penetratin rich clusters appeared and remained stable for several minutes. Then, they disappear by homogeneization of the GUV curvature and diffusion of penetration in about 5 seconds (Movie S1 in the supporting material). Second, penetratin induced two major alterations of the ^{31}P-NMR spectra of membranes comprised of five different compositions. 1) the presence of an isotropic peak indicating the formation of highly curved structures (Fig. 1, S1 and S2 in the supporting material) consistent with the vesiculation assumed from X ray diffraction base line distortion, and 2) two distinct peaks corresponding to lamellar structures were observed in PC, PC/PG and PC/SM/chol membranes (around 7.5 and 11 ppm) (Fig. 1c and S2). Noticeably, the isotropic component was observed at a peptide/lipid molar ratio (P/L 1/64) as shown in Fig S2. A clear phase separation was only observed at P/L of 1/32 but the broadening of the lamellar peak contribution was detected from P/L of 1/64. The resonances corresponding to lamellar structures were interpreted as two different regimes for phospholipids with lateral diffusion taking place on the distinct structures revealed by SAXS (L1 and L2 for PC/SM/Chol and L1 and L3 for PC/PG) and PC/PG GUV observation.

3.2. The arrangement of lipids is perturbed by penetratin

To better understand SAXS data showing that penetratin induced the formation of vesicles and phase separation, we have calculated and compared the electron density profiles for different lipid composition and temperatures. The value of the membrane phospholipid thickness (given as the P-P transversal distance) and of the hydration layer are reported in Table 1. In contrast with PC/PE and PC/SM/chol were penetratin induced only a small increase of the bilayer thickness, penetratin has split PC and PC/PG

membranes into two different structures (Fig. 2, table 1). For an arrangement (L1) the electron density profile is consistent with an increase of the hydration layer without significant effect on the bilayer thickness. L1 can be understood as the result of more water entering the inter-bilayer space under the osmotic influence of the peptide. However for the second arrangement detected (L3) the peptide addition induced a significant increase of both hydration and bilayer thickness (Fig. 2, table 1). Moreover, the thermal behavior reveals that the first arrangement (L1) is more temperature sensitive than the L3 arrangement (Fig. 2c). Noticeably, a small effect on membrane thickening and hydration increase was observed at P/L ratios of 1/64 (not shown), but the occurrence of the L3 arrangement was only observed at a P/L ratio of 1/32.

In PE membranes, a phospholipid which favors negative curvature, heating induced a transition from a lamellar to an inverted hexagonal phase H_{II} (Fig. 2d). In the presence of penetratin we observed the rise of three diffraction peaks which corresponds to a lamellar structure (L3). The electron density profile showed that the bilayer and the hydration thicknesses were increased (Table 1). In addition penetratin strongly reduces the capacity of PE to form inverse hexagonal phase as shown by the small peaks that were only detected at 45°C and suppressed the contribution of the cubic arrangement detected in the diffractogram.

To observe the membrane perturbations induced by the peptide we performed cryo-electron microscopy observations of LUV and MLV. In PC/PG LUV, the peptide induced membrane undulations and membrane adhesion (Fig. 3). The thickness of the penetratin-membrane bilayer complex at a high concentration of peptide was shown to be 7 nm by cryo-EM (Fig. S3). This distance is in agreement with the lamellar d-spacing measured by SAXS (7.05 nm).

3.3. Basic peptides induce membrane curvature.

The capability of penetratin to induce negatively curved structures was investigated by different approaches. As shown in Fig. 1c, S1 and S2, the ^{31}P-NMR spectra from different MLV show the characteristic asymmetrical line shape of a lamellar arrangement. The presence of penetratin induced the appearance of a strong isotropic signal suggesting highly curved phopholipid structures.

The formation of curved structures was observed in PC MLV by cryo-electron microscopy. Typical MLV smooth membranes are shown in the absence of the peptide

(Fig. S3c). In the presence of penetratin, many small vesicles of about 50 nm in diameter were observed (Fig. S3d).

A third evidence of peptide capacity to induce membrane curvature was obtained by direct observation of GUV. Penetratin induced the invagination of membranes and consequently the formation of tubes inside the GUV. These tubes experienced a dynamic evolution. Tubulation usually starts by invagination of thin tubes. After several minutes, the tube diameter increases to reach a size of about 2 μm. Then, a fluctuation period of tens of minutes resulted in tubular pearling (Fig. 4). The pearled structures remained stable for several minutes and then in less than five minutes evolved to a tube with bigger diameter. Pearling was not exclusive for penetratin and was also observed for the oligopeptide R9 (Fig. 4 and Movie S2). Pearling was observed in membranes composed of the zwitterionic phospholipid PC, as well as in the presence of a negative phospholipid (PC/PG, 9/1) and cholesterol (PC/Cholesterol, 8/1) GUV (Fig. S4). The relationship between the "wavelength" of the pearled tube (P) and the radius of the starting tube (Ro) were measured and analyzed with the equation $k=2\pi Ro/P$ [33]. The slope k is a factor related to the mechanism involved in pearling [34]. k=1 indicates an agent-induced pearling mechanism and k=0.7 a tension induced pearling. In the case of penetratin, we found k values from 1.01 to 1.07. For R9, the k values were more variable ranging from 1.0 to 1.3. However, in both cases, the k values were in agreement with a peptide mediated pearling as has been shown for other polymers [33]. The difference in k values between penetratin and R9 are related to the fact that the diameter of the tubes induced by R9 was usually smaller than those induced by penetratin. This suggests that R9 is able to induce stronger negative curvature compared to penetratin.

4. DISCUSSION

The molecular mechanisms of internalization of cell penetrating peptides are still controversial. Penetratin, Tat and polyarginine (R8) peptides had been shown to be internalized by endocytic and non endocytic pathways [11]. However, peptides actions in the cytoplasm and nucleus cannot be explained by endocytosis alone and require their translocation through the membrane phospholipid bilayer. Moreover, penetratin was shown to have an antimicrobial action against bacteria [23], organisms in which the plasma membrane is rich in PE and PG phospholipids. Some CPPs such as penetratin are part of protein transduction domains suggested to be involved not only in intracellular uptake but

also in extracellular export of transduction proteins. Thus, the interaction with the internal leaflet of the plasma membrane rich in PE and negatively charged phospholipids would be necessary for protein export. Therefore, we studied the modifications of lipid organization induced by penetratin on different phospholipids present in the outer and the inner leaflets of the eukaryotic plasma membrane.

The first important finding of this study is that penetratin is able to induce lamellar phase separation. This was clearly observed by X-ray suggested by the experiments with GUV and by NMR. Penetratin has been shown to perturb membranes in several ways such as in membrane packing [35] and thermal transitions [36]. To our knowledge, this is the first evidence of a clearly demonstrated (SAXS) lamellar phase separation induced by penetratin. The NMR spectra of PC, PC/PG and PC/SM/Chol showed that the peptide induced the separation of phospholipids with at least two different regimes. This phenomenon can be explained by two different hypotheses; first, the peptide might be able to separate phospholipid species resulting in bilayers of different composition. Second, the peptide-phospholipid interaction could induce a strong change in lipid diffusion. The peptide might simultaneously induce both phospholipid separation and slow down of lipid diffusion. A similar effect was observed for the peptide Tat with dimyristoyl-PC [37].

The second important finding is the increase of the hydration and bilayer thickness (table 1). An increase in the hydration zone induced by penetratin has been suggested previously [38]. The increase in the hydration layer is probably due to the accumulation of the peptide between the membrane bilayers as suggested by the dark bands between the membranes observed by cryo-EM. With PC, PC/PG and PE, the peptide induced a "new" lamellar phase with higher bilayer thickness and low thermal sensitivity indicating an increase in the rigidity of the membrane. One interesting point of this lamellar structure (L3) is that its intensity and amplitude are very different depending in lipid composition. In PC and PC/PG MLVs, the peaks are small. For MLV composed of PE the peaks were even higher than those corresponding to the lamellar phase. The fact that penetratin showed such a high and stable effect with PE, a phospholipid that induces negative curvature in membranes, is in agreement with the suggested action of penetratin as an agent that increases negative curvature. Why does the peptide induce negative curvature but does not favor the hexagonal phase? We propose that the growing process to form the long thin inverted cylinders is not favored by the peptide and only short rod-like structures are allowed, as was observed by cryo-fracture electron microscopy for Tat [37]. The increase in membrane thickness might correspond to the formation of distorted structures due to membrane

undulations [39]. These undulations could be analogous to the distorted lamellar structures reported by Tardieu [40]. The penetratin-induced membrane thickening is in contrast to the membrane thinning observed for the pore forming peptides alamethicin and melittin [41, 42].

The third important finding, the induction of membrane curvature was confirmed by direct cryo-electron microscopy observation of vesicles, curved structures and undulations. The capacity of basic peptides to induce negative membrane curvature is suggested to be the basis of the invagination and tubulation during "physical endocytosis" [20, 21]. Polylysine and Shiga toxin were also shown to be able to induce membrane invaginations [29, 43]. The reported decrease in the lamellar to hexagonal phase transition temperature induced by penetratin [44] is also consistent with the membrane negative curvature effect.

The fourth important finding was tube pearling. This is the first report on pearling induced by a molecule inside a membrane tube. The measured slope k suggests that pearling results by direct penetratin and R9 action. The exact mechanism of pearling is not clear at present. The peptide induces membrane negative curvature resulting in tubulation. After this first dynamic step, and to attain equilibrium, the peptide could detach from the membrane, change its conformation, or translocate through the bilayer. The consequent decrease in the quantity of membrane bound peptide could induce a change in tension resulting in pearling and in the decrease of the total negative curvature. The penetratin capacity to provoke changes in membrane tension is also suggested by the deformation of the GUV provoked by the unequal distribution of the peptide at the surface (Movie S1). It is known that the line tension at the boundary of domains results in bud formation, and the bud like structure observed was quite similar to those observed on GUV with coexisting fluid domains [45, 46].

Considering all these data we propose a model for penetratin action. As shown in Fig. 5, the first action of penetratin is its association to phospholipid head groups. Depending on the affinities between the peptide and the different phospholipids, penetratin is able to provoke phospholipid segregation and membrane thickening. Thereafter, the increase of peptide local concentration on separated membrane domains leads to membrane negative curvature resulting in undulations, vesiculation and/or tube formation and possibly inverse micelles.

How would these properties participate in the cellular uptake of penetratin and other basic peptides and in the export of transduction proteins? All the perturbations provoked by penetratin were observed at different degrees in membranes rich in lipids of the outer

leaflet and the inner leaflet of the plasma membrane suggesting a general mechanism of action. We propose that the lipid phase separation and the induction of negative curvature are keys to understand cellular uptake. First, the induction of invaginations and tubes observed in GUV could be a basis to explain the metabolic energy independent cellular "physical endocytosis" (for example at 4°C). This propensity to form invaginations can favor the metabolic endocytic processes (for example at 37°C). Secondly, once in the endosomes or at the surface of the plasma membrane, the high concentration of penetratin in concert with membrane potential and pH changes as well as lipid phase separation could induce a strong local negative curvature that might result in the formation of inverted micelle-like structures and, in fine, membrane translocation. The results showing that R9 produce thinner tubes [20] and smaller pearls (higher negative curvature) than penetratin are in correlation with comparative studies showing that R9 cellular uptake is more efficient than penetratin uptake [11, 47]. This correlation is in agreement with the prediction of the model that a peptide that induces higher negative curvature will be more efficient for membrane translocation. However, we cannot exclude the direct passage of the peptide across the membrane bilayer. The increase in membrane thickness may also suggest the inclusion of the peptide in the bilayer as suggested by Su et al. [17]. However, this interesting issue is beyond the scope of this study and will require further investigation.

5. Conclusion

The presented results show that penetratin is able to induce phase separation of phospholipids, the formation of vesicles, membrane undulations and tubular pearling. These data demonstrate its capacity to increase membrane negative curvature and suggest that dynamic phospholipids-penetratin complexes can be organized in different structural arrangements. It is interesting to speculate that these properties might be important to explain the cellular internalization by an endocytic-like mechanism independent of metabolic energy and also the formation of highly curved structures similar to the inverse micelles suggested to be the basis of membrane translocation (see figure S5).

Acknowledgements
Françoise Illien for technical help, Eric Dufourc for useful discussion of data and the X-ray diffraction facility at Spring8 (Japan). This work was supported by CNRS and an ANR-PCV grant.

REFERENCES

[1] G.P. Dietz, M. Bahr, Delivery of bioactive molecules into the cell: the Trojan horse approach, Mol Cell Neurosci 27 (2004) 85-131.
[2] M. Mae, U. Langel, Cell-penetrating peptides as vectors for peptide, protein and oligonucleotide delivery, Curr Opin Pharmacol 6 (2006) 509-514.
[3] C.L. Murriel, S.F. Dowdy, Influence of protein transduction domains on intracellular delivery of macromolecules, Expert Opin Drug Deliv 3 (2006) 739-746.
[4] J. Ayala, N. Touchot, A. Zahraoui, A. Tavitian, A. Prochiantz, The product of rab2, a small GTP binding protein, increases neuronal adhesion, and neurite growth in vitro, Neuron 4 (1990) 797-805.
[5] A. Prochiantz, Messenger proteins: homeoproteins, TAT and others, Curr Opin Cell Biol 12 (2000) 400-406.
[6] A. Joliot, C. Pernelle, H. Deagostini-Bazin, A. Prochiantz, Antennapedia homeobox peptide regulates neural morphogenesis, Proc Natl Acad Sci U S A 88 (1991) 1864-1868.
[7] F. Perez, P.M. Lledo, D. Karagogeos, J.D. Vincent, A. Prochiantz, J. Ayala, Rab3A and Rab3B carboxy-terminal peptides are both potent and specific inhibitors of prolactin release by rat cultured anterior pituitary cells, Mol Endocrinol 8 (1994) 1278-1287.
[8] D. Derossi, A.H. Joliot, G. Chassaing, A. Prochiantz, The third helix of the Antennapedia homeodomain translocates through biological membranes, J Biol Chem 269 (1994) 10444-10450.
[9] A. Ziegler, Thermodynamic studies and binding mechanisms of cell-penetrating peptides with lipids and glycosaminoglycans, Adv Drug Deliv Rev 60 (2008) 580-597.
[10] G. Drin, S. Cottin, E. Blanc, A.R. Rees, J. Temsamani, Studies on the internalization mechanism of cationic cell-penetrating peptides, J Biol Chem 278 (2003) 31192-31201.
[11] F. Duchardt, M. Fotin-Mleczek, H. Schwarz, R. Fischer, R. Brock, A comprehensive model for the cellular uptake of cationic cell-penetrating peptides, Traffic 8 (2007) 848-866.
[12] H. Binder, G. Lindblom, Charge-dependent translocation of the Trojan peptide penetratin across lipid membranes, Biophys J 85 (2003) 982-995.
[13] J.B. Rothbard, T.C. Jessop, R.S. Lewis, B.A. Murray, P.A. Wender, Role of membrane potential and hydrogen bonding in the mechanism of translocation of guanidinium-rich peptides into cells, J Am Chem Soc 126 (2004) 9506-9507.
[14] J.B. Rothbard, T.C. Jessop, P.A. Wender, Adaptive translocation: the role of hydrogen bonding and membrane potential in the uptake of guanidinium-rich transporters into cells, Adv Drug Deliv Rev 57 (2005) 495-504.
[15] D. Derossi, S. Calvet, A. Trembleau, A. Brunissen, G. Chassaing, A. Prochiantz, Cell internalization of the third helix of the Antennapedia homeodomain is receptor-independent, J Biol Chem 271 (1996) 18188-18193.
[16] R. Fischer, M. Fotin-Mleczek, H. Hufnagel, R. Brock, Break on through to the other side-biophysics and cell biology shed light on cell-penetrating peptides, Chembiochem 6 (2005) 2126-2142.
[17] Y. Su, R. Mani, M. Hong, Asymmetric insertion of membrane proteins in lipid bilayers by solid-state NMR paramagnetic relaxation enhancement: A cell-penetrating peptide example, Journal of the American Chemical Society 130 (2008) 8856-8864.
[18] P.E. Thoren, D. Persson, M. Karlsson, B. Norden, The antennapedia peptide penetratin translocates across lipid bilayers - the first direct observation, FEBS Lett 482 (2000) 265-268.
[19] D. Persson, P.E. Thoren, E.K. Esbjorner, M. Goksor, P. Lincoln, B. Norden, Vesicle size-dependent translocation of penetratin analogs across lipid membranes, Biochim Biophys Acta 1665 (2004) 142-155.
[20] A. Lamaziere, F. Burlina, C. Wolf, G. Chassaing, G. Trugnan, J. Ayala-Sanmartin, Non-metabolic membrane tubulation and permeability induced by bioactive peptides, PLoS ONE 2 (2007) e201.
[21] A. Lamaziere, C. Wolf, O. Lambert, G. Chassaing, G. Trugnan, J. Ayala-Sanmartin, The homeodomain derived peptide Penetratin induces curvature of fluid membrane domains, PLoS ONE 3 (2008) e1938.

[22] A. Lamaziere, G. Chassaing, G. Trugnan, J. Ayala-Sanmartin, Tubular structures in heterogeneous membranes induced by the cell penetrating peptide penetratin, Commun Integr Biol 2 (2009) 223-224.
[23] W.L. Zhu, S.Y. Shin, Antimicrobial and cytolytic activities and plausible mode of bactericidal action of the cell penetrating peptide penetratin and its lys-linked two-stranded peptide, Chem Biol Drug Des 73 (2009) 209-215.
[24] J. Ayala-Sanmartin, M. Zibouche, F. Illien, M. Vincent, J. Gallay, Insight into the location and dynamics of the annexin A2 N-terminal domain during Ca(2+)-induced membrane bridging, Biochim Biophys Acta 1778 (2008) 472-482.
[25] C. Tessier, P. Quinn, K. Koumanov, G. Trugnan, D. Rainteau, C. Wolf, Modulation of the phase heterogeneity of aminoglycerophospholipid mixtures by sphingomyelin and monovalent cations: maintenance of the lamellar arrangement in the biological membranes, Eur Biophys J 33 (2004) 513-521.
[26] T.J. McIntosh, K.G. Kulkarni, S.A. Simon, Membrane fusion promoters and inhibitors have contrasting effects on lipid bilayer structure and undulations, Biophys J 76 (1999) 2090-2098.
[27] O. Lambert, N. Cavusoglu, J. Gallay, M. Vincent, J.L. Rigaud, J.P. Henry, J. Ayala-Sanmartin, Novel organisation and properties of annexin 2-membrane complexes, J Biol Chem 279 (2004) 10872-10882.
[28] J. Dubochet, M. Adrian, J.J. Chang, J.C. Homo, J. Lepault, A.W. McDowall, P. Schultz, Cryo-electron microscopy of vitrified specimens, Q Rev Biophys 21 (1988) 129-228.
[29] F.M. Menger, V.A. Seredyuk, M.V. Kitaeva, A.A. Yaroslavov, N.S. Melik-Nubarov,Migration of poly-L-lysine through a lipid bilayer, J Am Chem Soc 125 (2003) 2846-2847.
[30] A. Lamaziere, G. Chassaing, G. Trugnan, J. Ayala-Sanmartin, [Transduction peptides: structural-functional analyses in model membranes], J Soc Biol 200 (2006) 229-233.
[31] M. Gandhavadi, D. Allende, A. Vidal, S.A. Simon, T.J. McIntosh, Structure, composition, and peptide binding properties of detergent soluble bilayers and detergent resistant rafts, Biophys J 82 (2002) 1469-1482.
[32] C. Tessier, P. Nuss, G. Staneva, C. Wolf, Modification of membrane heterogeneity by antipsychotic drugs: an X-ray diffraction comparative study, J Colloid Interface Sci 320 (2008) 469-475.
[33] I. Tsafrir, D. Sagi, T. Arzi, M.A. Guedeau-Boudeville, V. Frette, D. Kandel, J. Stavans, Pearling instabilities of membrane tubes with anchored polymers, Phys Rev Lett 86 (2001) 1138-1141.
[34] P. Nelson, T. Powers, U. Seifert, Dynamical Theory of the Pearling Instability in Cylindrical Vesicles, Phys Rev Lett 74 (1995) 3384-3387.
[35] Z. Salamon, G. Lindblom, G. Tollin, Plasmon-waveguide resonance and impedance spectroscopy studies of the interaction between penetratin and supported lipid bilayer membranes, Biophys J 84 (2003) 1796-1807.
[36] I.D. Alves, I. Correia, C.Y. Jiao, E. Sachon, S. Sagan, S. Lavielle, G. Tollin, G. Chassaing, The interaction of cell-penetrating peptides with lipid model systems and subsequent lipid reorganization: thermodynamic and structural characterization, J Pept Sci 15 (2009) 200-209.
[37] S. Afonin, A. Frey, S. Bayerl, D. Fischer, P. Wadhwani, S. Weinkauf, A.S. Ulrich, The cell-penetrating peptide TAT(48-60) induces a non-lamellar phase in DMPC membranes, Chemphyschem 7 (2006) 2134-2142.
[38] G. Fragneto, F. Graner, T. Charitat, P. Dubos, E. Bellet-Amalric, Interaction of the third helix of Antennapedia homeodomain with a deposited phospholipid bilayer: A neutron reflectivity structural study, Langmuir 16 (2000) 4581-4588.
[39] J.F. Nagle, S. Tristram-Nagle, Structure of lipid bilayers, Bba-Rev Biomembranes 1469 (2000) 159-195.
[40] A. Tardieu, V. Luzzati, F.C. Reman, Structure and Polymorphism of Hydrocarbon Chains of Lipids - Study of Lecithin-Water Phases, Journal of Molecular Biology 75 (1973) 711-&.
[41] F.Y. Chen, M.T. Lee, H.W. Huang, Evidence for membrane thinning effect as the mechanism for peptide-induced pore formation, Biophys J 84 (2003) 3751-3758.

[42] M.T. Lee, W.C. Hung, F.Y. Chen, H.W. Huang, Many-body effect of antimicrobial peptides: on the correlation between lipid's spontaneous curvature and pore formation, Biophys J 89 (2005) 4006-4016.
[43] W. Romer, L. Berland, V. Chambon, K. Gaus, B. Windschiegl, D. Tenza, M.R. Aly, V. Fraisier, J.C. Florent, D. Perrais, C. Lamaze, G. Raposo, C. Steinem, P. Sens, P. Bassereau, L. Johannes, Shiga toxin induces tubular membrane invaginations for its uptake into cells, Nature 450 (2007) 670-675.
[44] I.D. Alves, N. Goasdoue, I. Correia, S. Aubry, C. Galanth, S. Sagan, S. Lavielle, G. Chassaing, Membrane interaction and perturbation mechanisms induced by two cationic cell penetrating peptides with distinct charge distribution, Biochim Biophys Acta 1780 (2008) 948-959.
[45] T. Baumgart, S.T. Hess, W.W. Webb, Imaging coexisting fluid domains in biomembrane models coupling curvature and line tension, Nature 425 (2003) 821-824.
[46] A.J. Garcia-Saez, S. Chiantia, P. Schwille, Effect of line tension on the lateral organization of lipid membranes, J Biol Chem 282 (2007) 33537-33544.
[47] F. Burlina, S. Sagan, G. Bolbach, G. Chassaing, Quantification of the cellular uptake of cell-penetrating peptides by MALDI-TOF mass spectrometry, Angew Chem Int Ed Engl 44 (2005) 4244-4247.

FIGURES

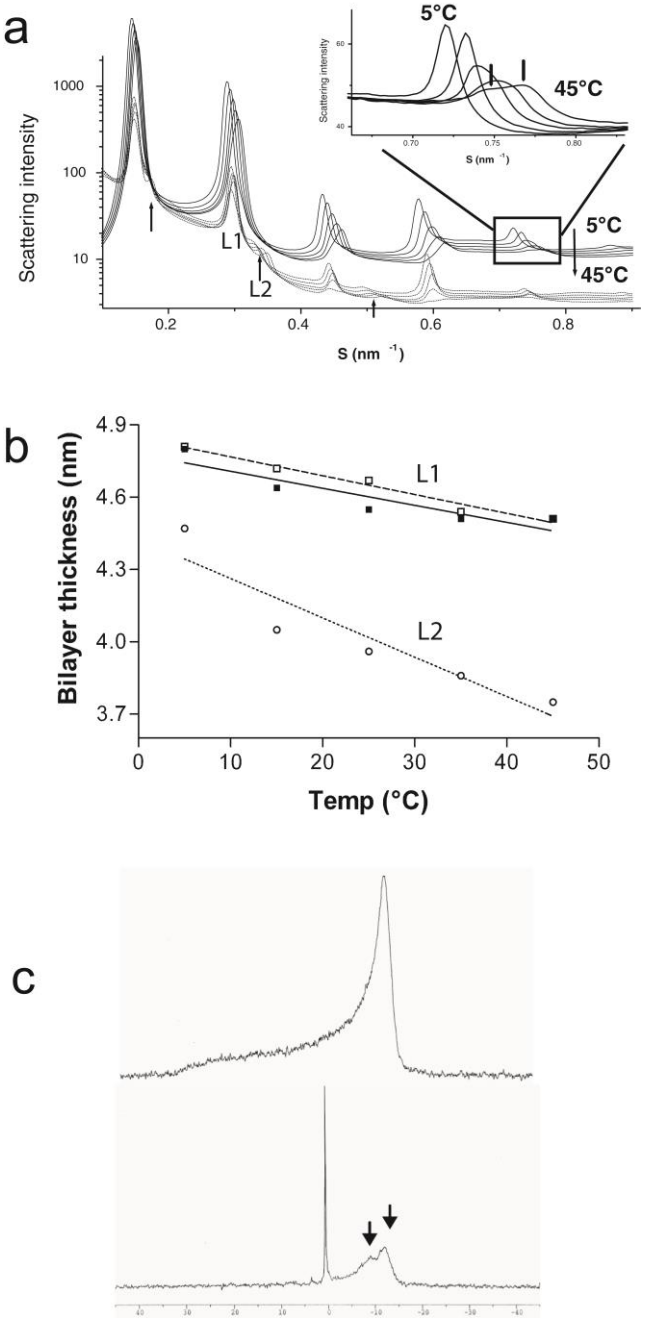

Figure 1. Penetratin induces phospholipid phase separation. (a), Series SAXS diffractograms at 10°C interval obtained from 5°C (top) to 45°C (bottom). PC/SM/Chol (1/1/1) MLV in the absence (continuous lines) and presence of penetratin (dotted lines). Penetratin induced lamellar phase separation (arrows). Inset, amplification of the fifth order peak in the absence of penetratin. Arrows indicate the separation of two lamellar phases at 45°C. (b), Temperature dependence of the membrane bilayer thickness of PC/SM/chol in the absence of peptide L1 (■), and the L1 (□) and the L2 (○) lamellar phases in the presence of penetratin. (c), ^{31}P-NMR spectra of PC/SM/chol MLV in the absence (top) and the presence of penetratin (bottom). The split peak (arrows) suggests separation of two phases coexisting with an isotropic component (resonance at 0ppm).

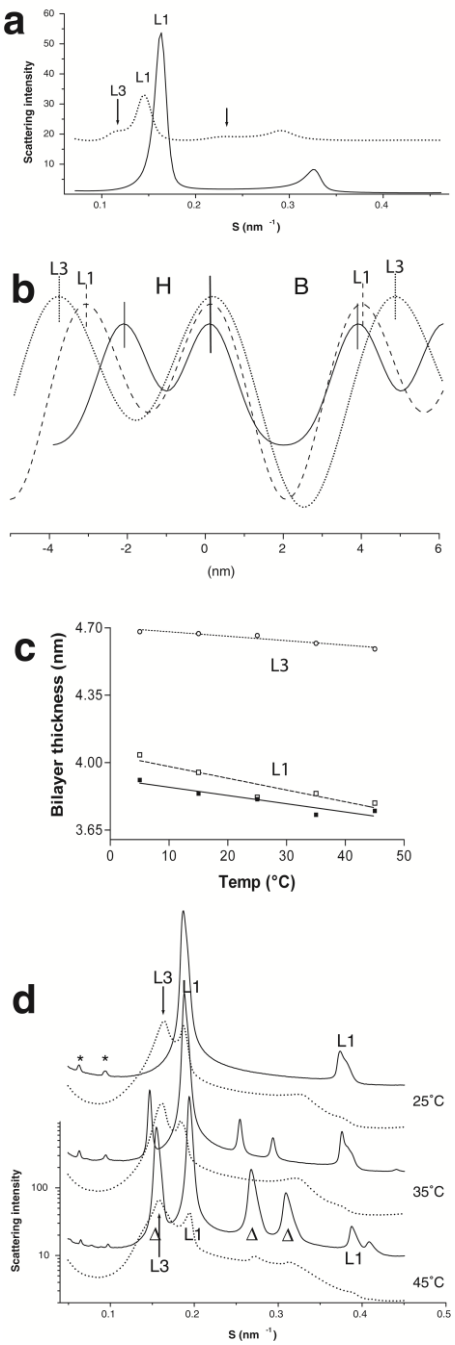

Figure 2. Penetratin induces specific arrangements of phospholipids. (a), SAXS diffractograms of PC MLV in the absence (continuous line) and the presence of penetratin (dotted line). In PC/PG (9/1), penetratin induced a shift of the d-spacing of the lamellar phase peak (L1) from 6.0 to 7.1, and a minor component appears (L3, d-spacing of 8.5; arrows). (b), Electron density profiles of lamellar phases of PC at 25°C in the absence (continuous line) and the presence of penetratin. Principal lamellar phase L1 (dashed line), thick lamellar phase L3 (dotted line). H; hydration distance, B; bilayer distance. (c), Temperature dependency of the membrane bilayer thickness of PC in the absence of penetratin (■) and the L1 lamellar phase (□) and the lamellar phase L3 (○) in the presence of penetratin. (d), in PE the inverted hexagonal phase peaks are shown at 35°C and 45°C (arrowheads Δ). In the presence of penetratin the lamellar phase peaks (L1) decrease in intensity and the peaks corresponding to a cubic phase (*) disappear. A small inverted hexagonal phase was detected only at 45°C and new peaks corresponding to the lamellar phase L3 are predominant at all temperatures (arrows).

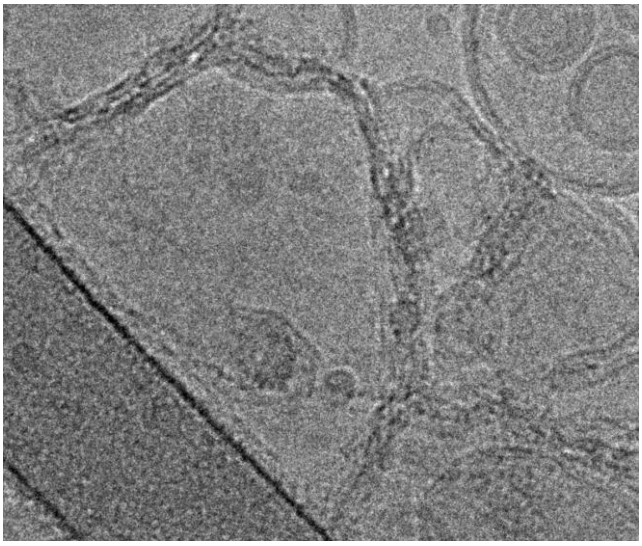

Figure 3. Membrane undulations provoked by penetratin. Cryo-electron microscopy images of PC/PG LUV incubated with penetratin. Notice the peptide-induced membrane perturbations including undulations, bridging and induction of membrane-peptide heterogeneity as revealed by the difference in electron density of the membrane. Bar 50 nm.

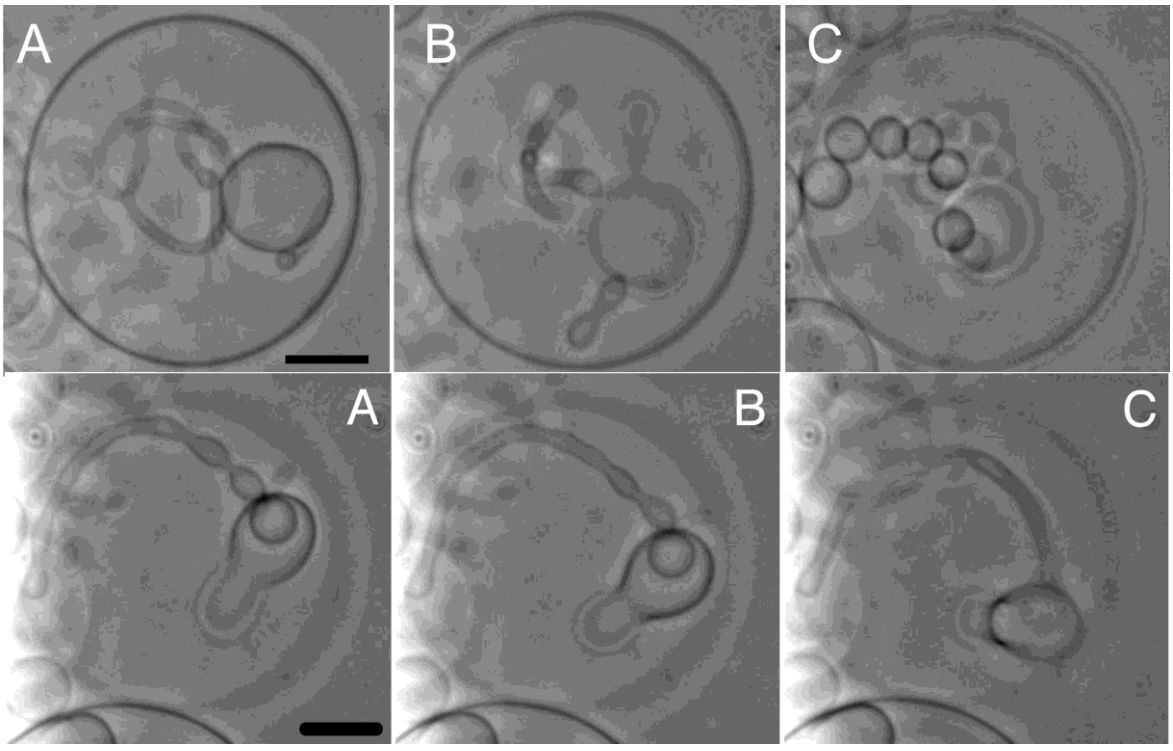

Figure 4. Reversibility of membrane pearling in tubes. Top: Time lapse images of pearling in tubes (PC GUV) incubated with penetratin (A; t = 0 min, B; t = 30 min, C; t = 56 min). Bottom: Time lapse images of de-pearling in tubes (PC GUV) incubated with R9 (A; t = 0 s, B; t = 45 s, C; t = 120 s). Bars 10 μm. See also supplementary movie 2.

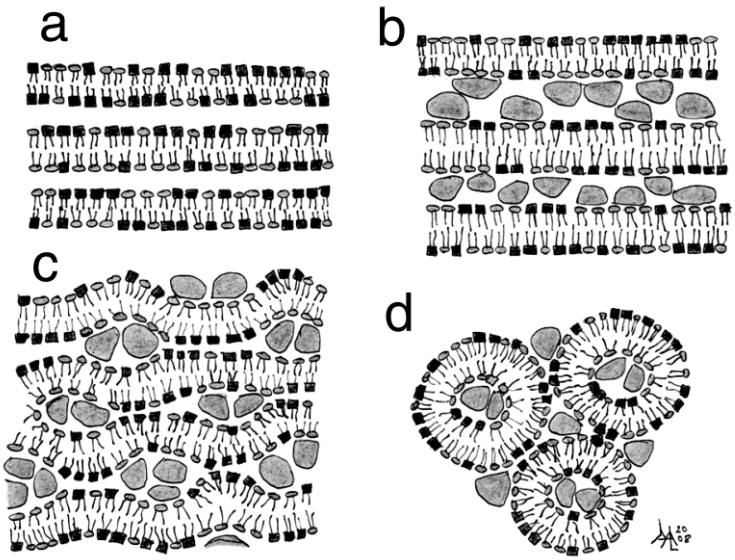

Figure 5. Model for penetratin and basic peptides induced membrane perturbations and translocation. Lipid fluid membrane composed of different lipids (gray circles and black squares) (a). In contact with penetratin, the membrane experiments lipid phase separation, membrane adhesion and bilayer thickening (b). After phase separation in different membrane domains, the rise in peptide concentration results in induction of negative curvature containing structures including undulations (c), that lead to the formation of small vesicles (d). The increase in membrane curvature might lead to the formation of inverse micelles that had been suggested to be necessary for membrane translocation. A schematic representation of the relationship of the obtained data with the model is illustrated in Fig. S5.

Table 1. Thickness of membrane bilayer and hydration layer of the lamellar phases for different lipid compositions in the presence and absence of penetratin at 25°C and 45°C.

Lipid composition	temperature 25°C									
	Bilayer (nm)					Hydration (nm)				
	none		+ penetratin			none		+ penetratin		
	L1	L2	L1	L2	L3	L1	L2	L1	L2	L3
PC/SM/Chol	4.55		4.67	3.96		2.17		2.01	1.98	
PC	3.81		3.82		4.66	2.19		3.21		3.96
PC/PG	3.86		3.83		4.58	2.30		3.06		3.80
PC/PE	3.92		4.01			2.02		2.25		
PE	3.88	3.74	3.84		4.21	1.47	1.53	1.49		1.86
	temperature 45°C									
PC/SM/Chol	4.51	4.14	4.50	3.75		2.05	2.57	2.00	1.98	
PC	3.75		3.79		4.59	2.14		2.95		3.77
PC/PE	3.89		4.02			2.02		2.26		